Supporting Information

Dissecting the Innate Immune Recognition of Opioid Inactive Isomer (+)-Naltrexone Derived Toll-like Receptor 4 (TLR4) Antagonists

Xiaozheng Zhang[1, 2], Fengchao Cui*[,3], Hongqian Chen[1], Tianshu Zhang[1], Kecheng Yang[3], Yibo Wang[1], Zhenyan Jiang[4], Kenner C. Rice[5], Linda R. Watkins[6], Mark R Hutchinson[7], Yunqi Li[3], Yinghua Peng[8], Xiaohui Wang*[,1]

[1]Laboratory of Chemical Biology, Changchun Institute of Applied Chemistry, Chinese Academy of Sciences, Changchun, Jilin, 130022, China; University of Chinese Academy of Sciences, Beijing, 100039, China

[2]State Key Laboratory of Natural Medicines, China Pharmaceutical University, Nanjing, 210009, China

[3]Key Laboratory of Synthetic Rubber, Changchun Institute of Applied Chemistry, Chinese Academy of Sciences, Changchun, Jilin, 130022, China

[4]School of Pharmaceutical Sciences, Jilin University, Changchun, Jilin, 130021, China

[5]Drug Design and Synthesis Section, National Institute on Drug Abuse and National Institute on Alcohol Abuse and Alcoholism, National Institutes of Health, Rockville, MD 20892, USA

[6]Department of Psychology and Neuroscience, and the Center for Neuroscience, University of Colorado at Boulder, Boulder, CO 80309, USA

[7]Discipline of Physiology, Adelaide Medical School, University of Adelaide, South Australia, Australia; ARC Centre of Excellence for Nanoscale Biophotonics, University of Adelaide, South Australia, 5000, Australia.

[8]State Key Laboratory for Molecular Biology of Special Economic Animals, Institute of Special Wild Economic Animals and Plants, Chinese Academy of Agricultural Sciences, Changchun, Jilin 130112, China

* Corresponding author
E-mail: fccui@ciac.ac.cn
E-mail: xiaohui.wang@ciac.ac.cn

Table S1. The decomposition of per-residue binding free energies (kcal/mol) of TLR4 antagonists binding to MD-2

	Compound				
Residue	**1**	**2**	**3**	**4**	**5**
Ser48	-1.5 (0.9)				
Ile52	-1.4 (0.3)	-2.3 (0.5)	-1.5 (0.3)		-1.6 (0.4)
Val61	-1.6 (0.4)	-1.2 (0.3)			-1.3 (0.3)
Phe76	-2.1 (0.4)	-1.7 (0.4)	-2.4 (0.3)	-2.5 (0.3)	-3.0 (0.4)
Leu78		-1.4 (0.3)	-1.0 (0.3)		
Glu92	-1.5 (0.4)	-1.5 (0.7)	-2.2 (1.0)	-1.5 (0.5)	
Leu94			-2.2 (0.7)	-2.2 (0.6)	-0.9 (0.2)
Pro118				-2.0 (0.4)	
Phe119	-2.2 (0.4)	-1.5 (0.4)	-2.6 (0.5)	-3.8 (0.5)	-2.3 (0.5)
Phe121	-1.5 (0.5)	-1.1 (0.3)	-2.9 (0.6)		
Phe147					-2.0 (0.7)
Cys148					-1.3 (0.3)
Leu149	-0.7 (0.2)				-2.1 (0.5)
Phe151	-2.7 (0.5)	-2.2 (0.5)	-2.4 (0.5)		-0.9 (0.4)

Numbers in parentheses present standard error

Table S2. Hydrogen bonding interactions of key residues Arg90 and Glu122 and the corresponding probabilities in state I, II and III over the MD simulations

System			state		
	Donor	Acceptor	I	II	III
apo-MD-2	:90:N	:78:O	1	0.99	0.98
	:78:O	:90:N	1	0.98	0.95
	:122:OE1	:90:NH2	0	0	0.21
	:122:OE2	:90:NH2	0	0	0.18
	:122:OE1	:90:NH1	0	0	0.17
	:122:OE2	:90:NH1	0	0	0.15
lip-MD-2	:78:O	:90:N	1	N/A	N/A
	:90:N	:78:O	0.99	N/A	N/A
1-MD-2	:90:N	:78:O	1	0.99	0.99
	:78:O	:90:N	1	0.80	0.93
2-MD-2	:90:N	:78:O	1	0.99	1
	:78:O	:90:N	0.98	0.98	0.97
	:122:OE2	:90:NH1	0	0.25	0
	:122:OE1	:90:NH1	0	0.22	0.22
	:122:OE1	:90:NH2	0	0.17	0.17
	:122:OE2	:90:NH2	0	0.16	0.23
3-MD-2	:90:N	:78:O	1	1	1
	:78:O	:90:N	1	0.97	0.86
	:122:OE2	:90:NH1	0	0.40	0
	:122:OE2	:90:NH2	0	0.38	0.19
	:122:OE1	:90:NH1	0	0.26	0
	:122:OE1	:90:NH2	0	0.21	0.26
4-MD-2	:90:N	:78:O	1	1	0.95
	:78:O	:90:N	0.99	0.98	0.92
	:122:OE2	:90:NH2	0	0	0.27
	:122:OE2	:90:NH1	0	0	0.27
	:122:OE1	:90:NH2	0	0	0.18
	:122:OE1	:90:NH1	0	0	0.18
5-MD-2	:78:O	:90:N	0.97	0.79	0
	:90:N	:78:O	0.88	0.83	0
	:122:OE1	:90:NH1	0	0.18	0.62
	:122:OE2	:90:NH2	0	0.14	0.66
	:122:OE1	:90:NH2	0	0.10	0.61
	:122:OE2	:90:NH1	0	0.12	0.55

Hydrogen bonds were determined by the criteria of $\leq$ 3.5 Å between donor and acceptor and $\geq$ 120° angle between donor-H-acceptor.

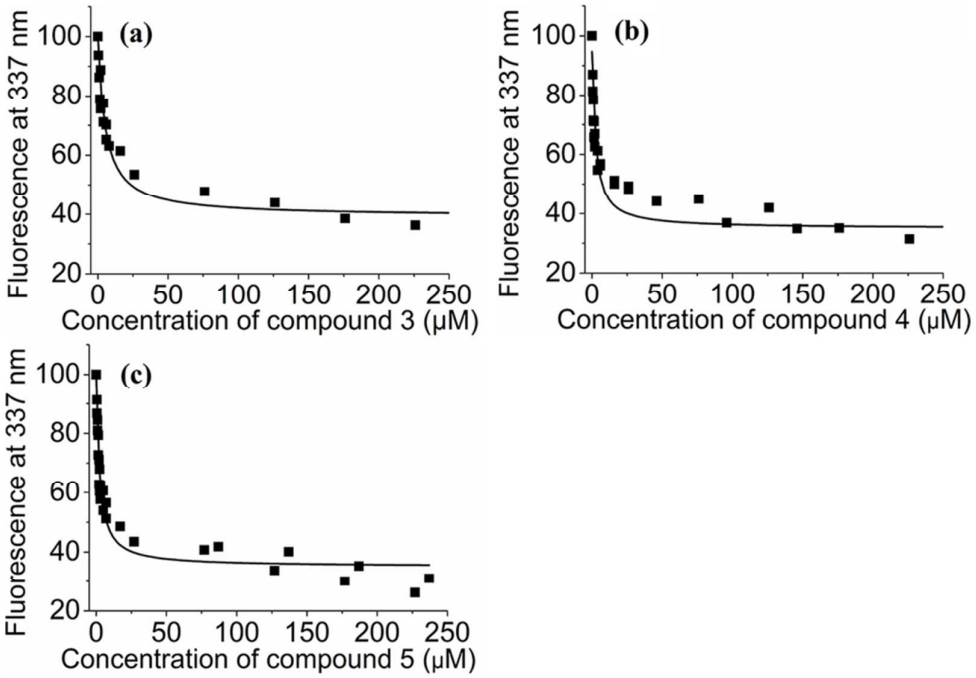

Figure S1. Titration curves of **3** (a), **4** (b) and **5** (c) binding to MD-2. 295 nm was chosen as the excitation of MD-2 intrinsic Trp fluorescence and emission at 337 nm (peak position) was plotted against the titrated compound concentration. By fitting the curves by nonlinear least-square regression, the K_d of 5.0 ± 0.8 μM (**3**), 2.3 ± 0.6 μM (**4**) and 2.1 ± 0.3 μM (**5**) are obtained. It should be noted that the titration of (+)-N-methylnaltrexone (**6**) with MD-2 binding was also performed similarly. The titration of **6** is far away from reaching a stable plateau phase, which prevents the quantitatively fitting of dissociation constant (> 40 μM) of **6** binding to MD-2.

.

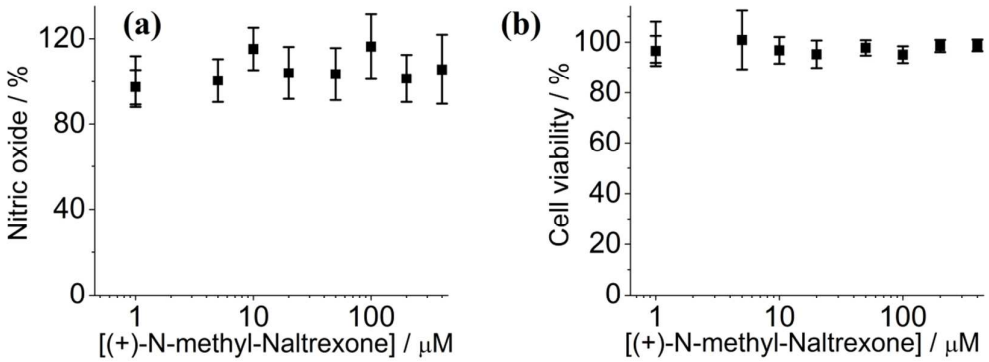

Figure S2. TLR4 antagonist activity and cellular toxicity of (+)-N-methylnaltrexone (**6**). **6** has no TLR4 antagonist activity (IC_{50} > 400 μM). **6** did not inhibit LPS induced TLR4 signaling nitric oxide (NO) production (a), and showed no apparent cellular toxicity (b). Cellular viability was determined by crystal violet staining method.

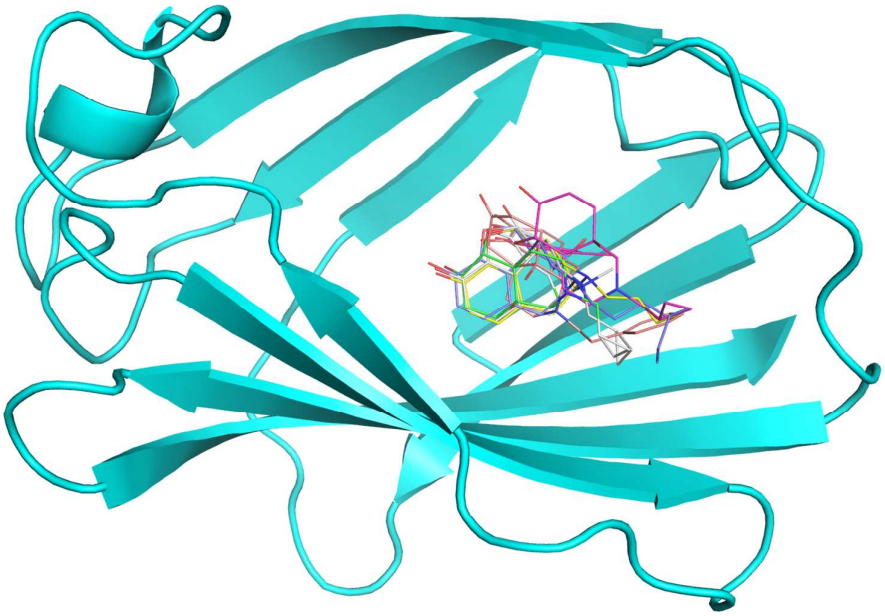

Figure S3. The best docking poses of **1** (green), **2** (yellow), **3** (salmon), **4** (cyan), **5** (magenta) and **6** (grey). Ligands are shown as lines and MD-2 is shown as cartoon

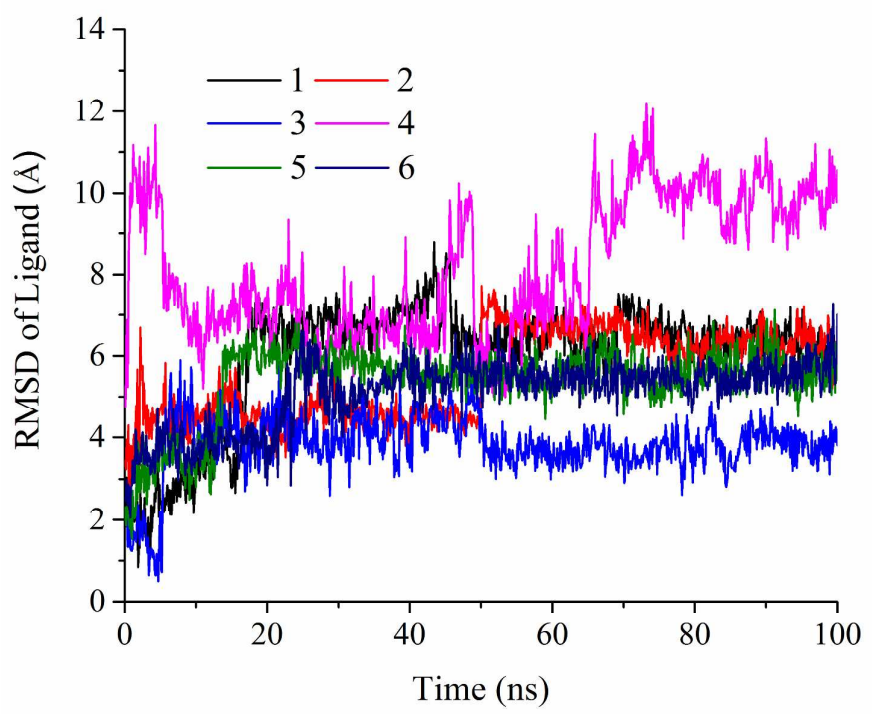

Figure S4. Time evolution of ligand RMSD. Black, red, blue, magenta, dark green and navy indicate MD-2 in the complex with **1**, **2**, **3**, **4**, **5** and **6** respectively.

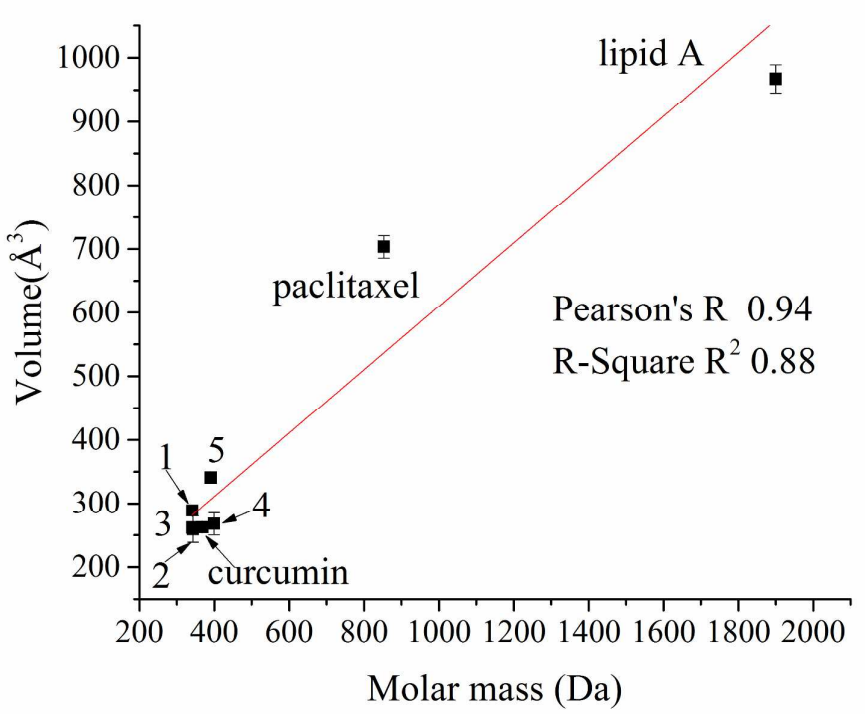

Figure S5. Correlation of the MD-2 cavity volume with the molar mass of the ligands.

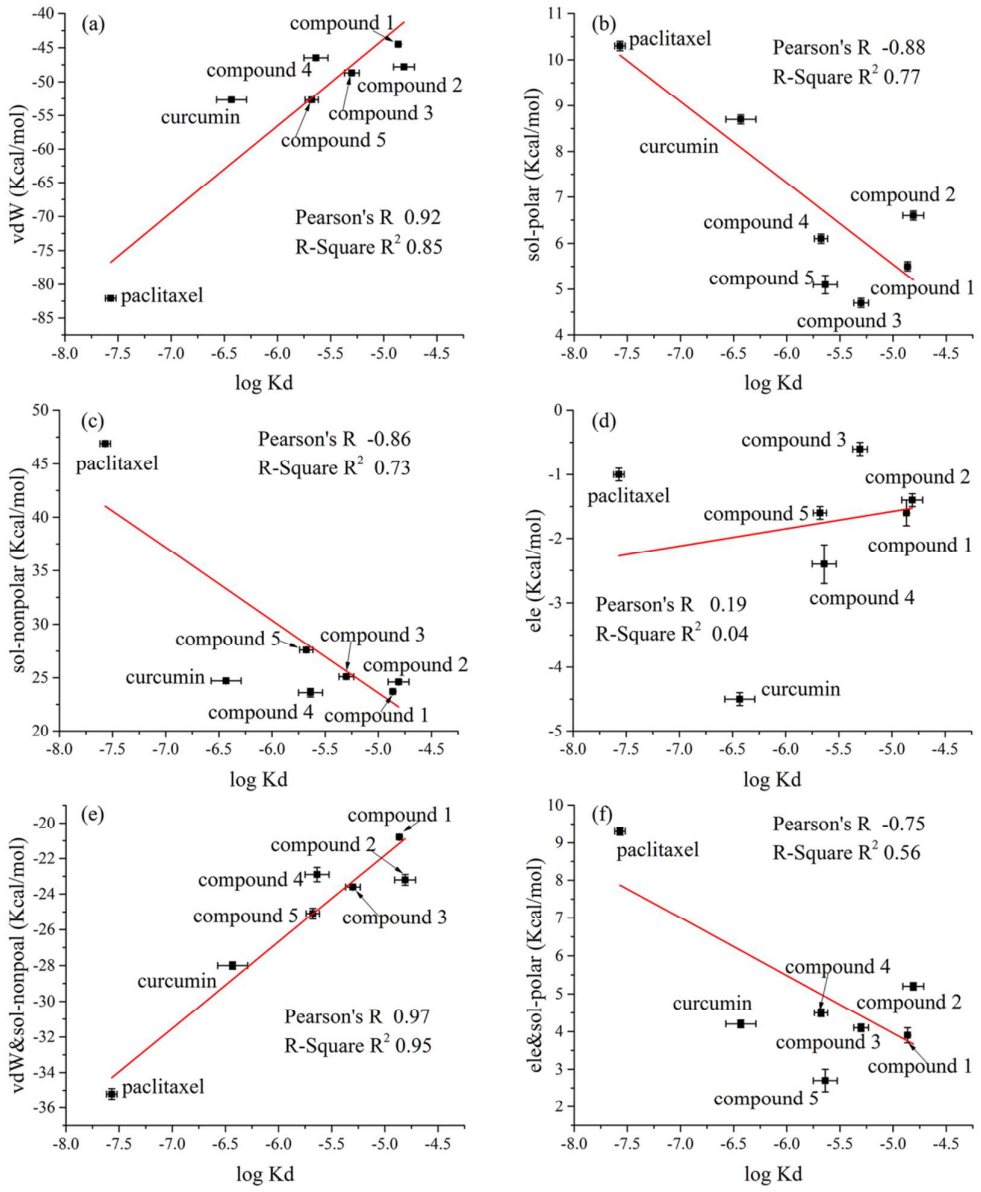

Figure S6. Correlation of the logarithm of experimentally determined dissociation constants log K_d with the decomposition of binding free energies: (a) van der Waals interactions (vdW) versus log K_d; (b) polar solvation free energy (sol-polar) versus log K_d; (c) non-polar solvation free energy (sol-nonpolar) versus log K_d; (d) electrostatic interactions (ele) versus log K_d; (e) van der Waals interactions and the non-polar salvation free energy (vdW & sol-nonpolar) versus log K_d; (f) electrostatic interactions and polar salvation free energy (ele & sol-polar) versus log K_d.

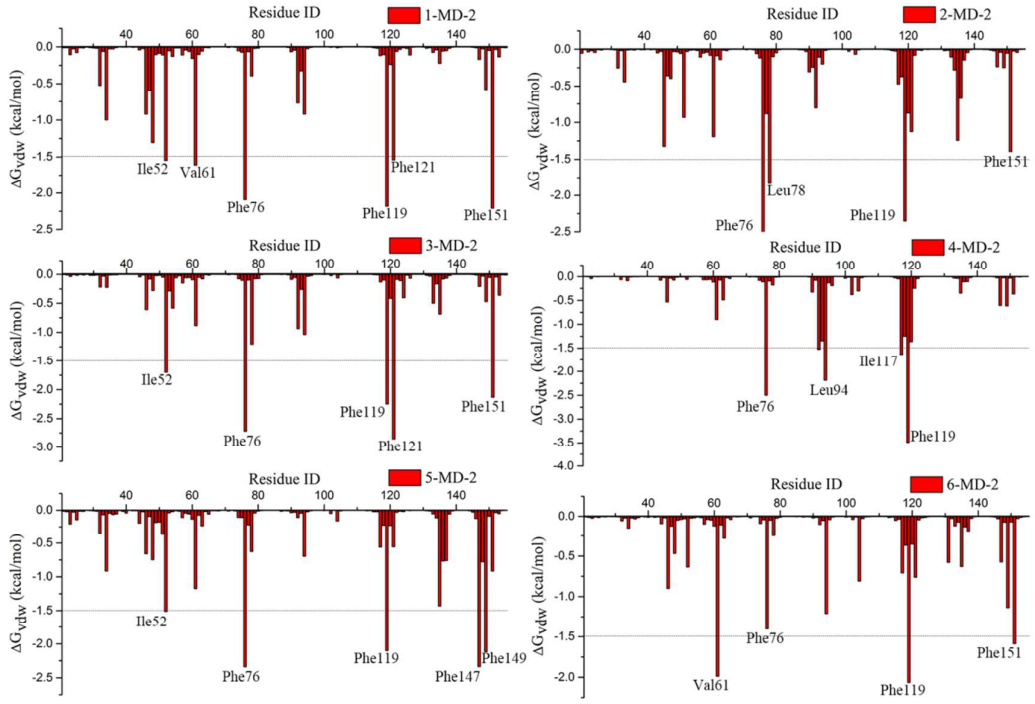

Figure S7. Analysis of the van der Waals contribution of each residue in binding free energy. Residues with ΔG_{vdw}> 1.5 Kcal/mol are labeled.

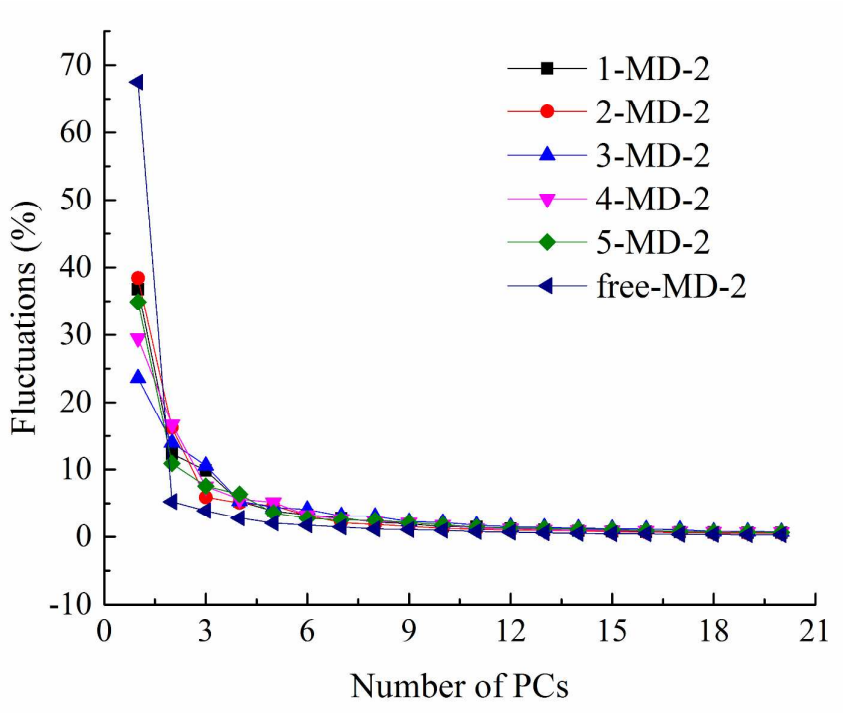

Figure S8. Percentages of fluctuations captured by Cartesian-coordinate PCs for all systems. Black, red, blue, magenta, dark green and navy indicate MD-2 in the complex with **1**, **2**, **3**, **4**, **5** and **6** respectively.

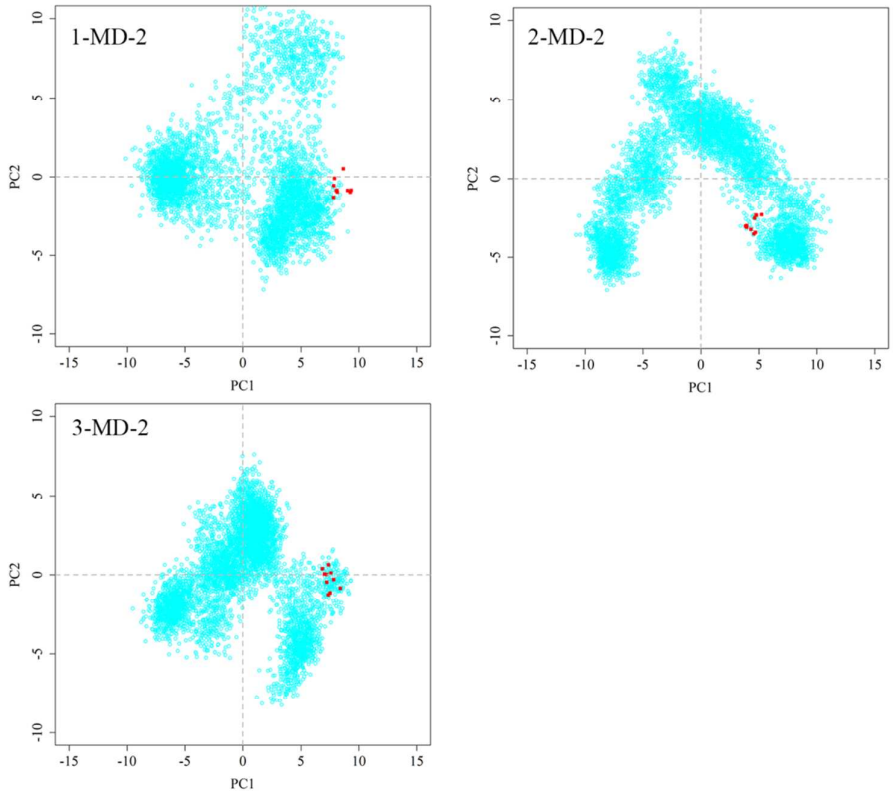

Figure S9. PCA analysis of **1**-MD-2, **2**-MD-2 and **3**-MD-2. Ten crystallographic MD-2 structures are colored red while the distribution of MD conformers is depicted with cyan points.

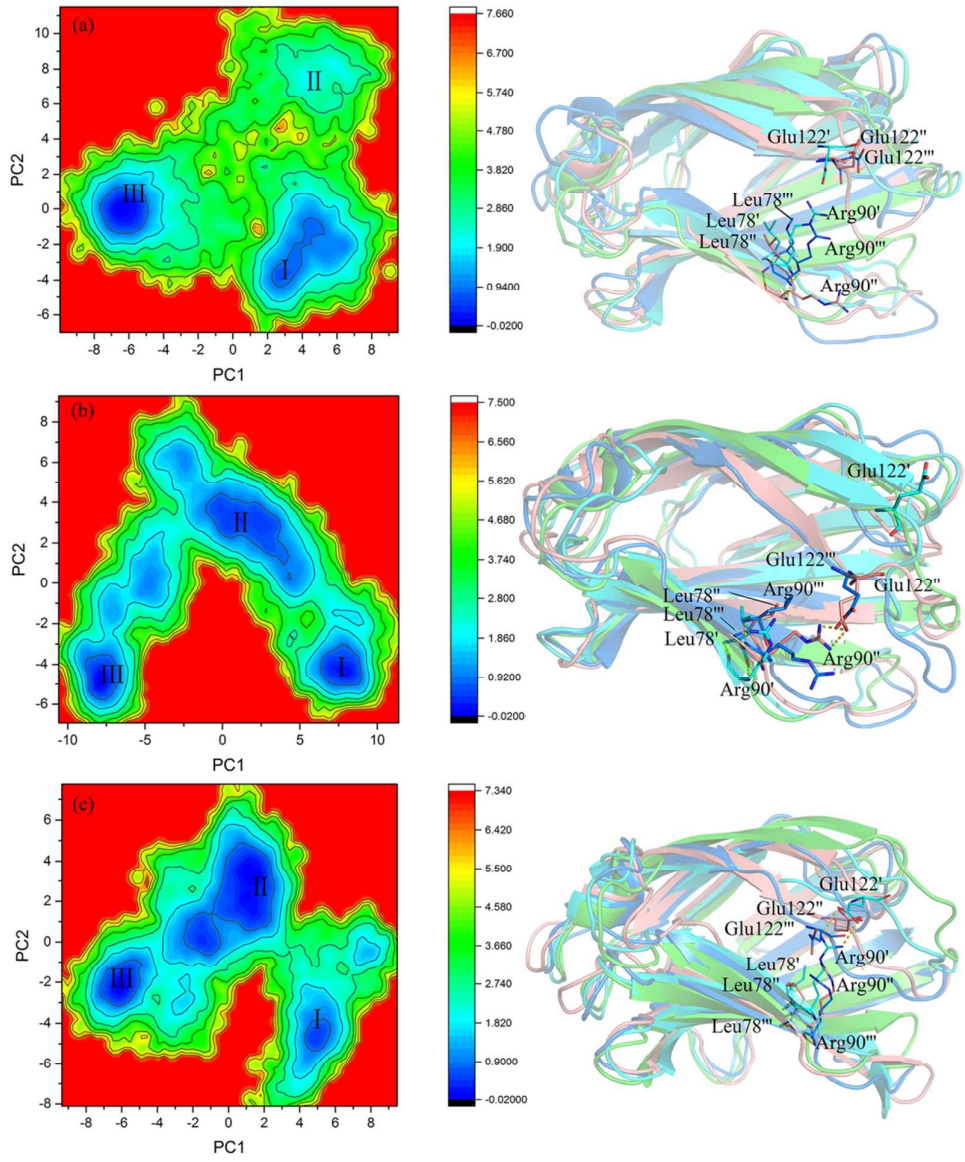

Figure S10. FEL analysis of MD trajectories of **1**-MD-2 (a), **2**-MD-2 (b) and **3**-MD-2 (c). The representative MD-2 structures corresponding to each FEL state are also shown. State I: cyan color; State II, salmon color; State III, marine color. Key residues involving hydrogen bond interactions at the mouth of MD-2 cavity are shown as stick. Free energy values are given in kcal/mol as indicated by the color bars.

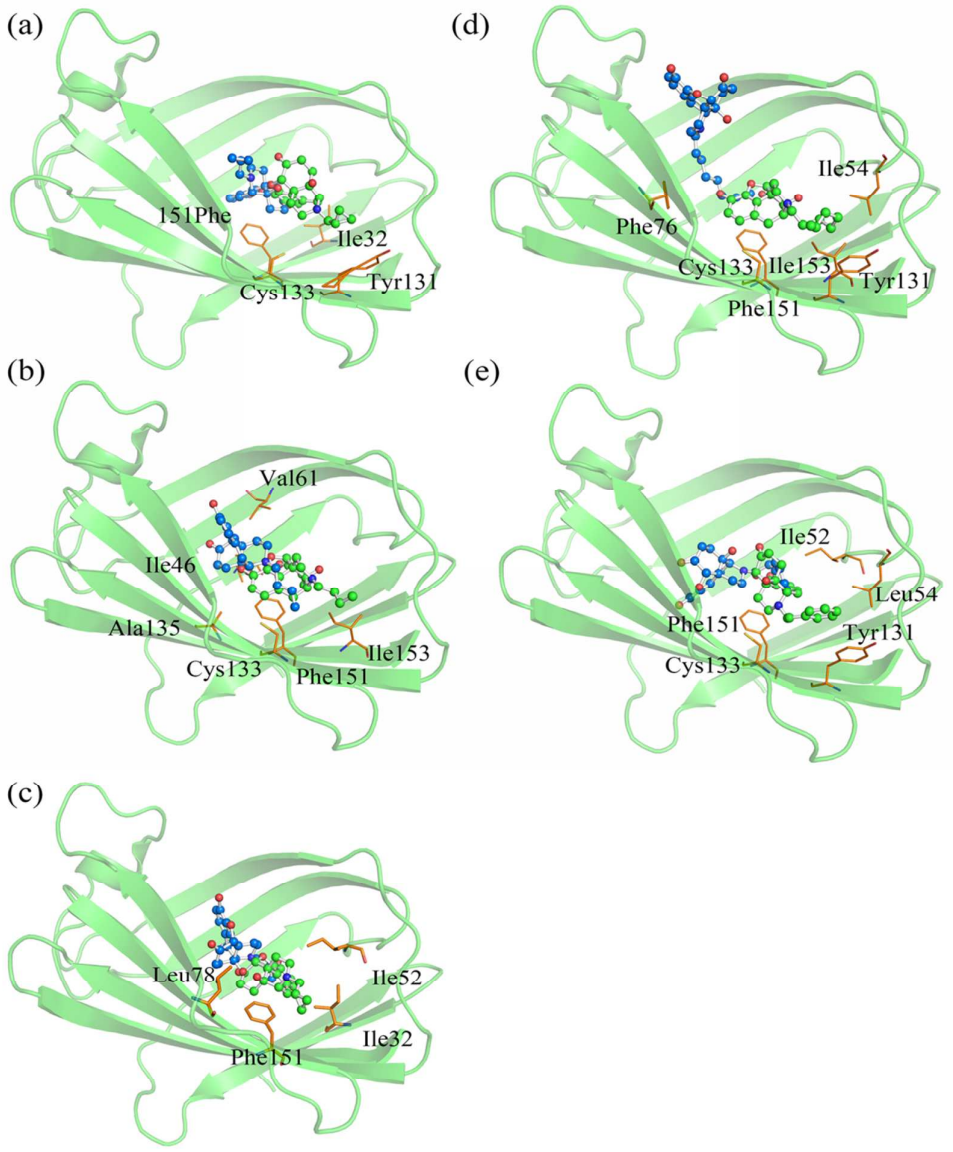

Figure S11. Alignments of the best docking poses (green ball and stick) and the poses in the representative MD-2 binding structure with the lowest-energy (navy ball and stick) of **1** (a), **2** (b), **3** (c), **4** (d) and **5** (e). The green cartoon represented the initial MD-2 structures.